Progress in Neuropsychopharmacology & Biological Psychiatry 98 (2020) 109819

Contents lists available at ScienceDirect

Progress in Neuropsychopharmacology & Biological Psychiatry

journal homepage: www.elsevier.com/locate/pnp

Rumination network dysfunction in major depression: A brain connectome study

Ruibin Zhang[a,b,c,d], Georg S. Kranz[a,e,f], Wenjin Zou[g], Yue Deng[h], Xuejun Huang[h], Kangguang Lin[i,j,**], Tatia M.C. Lee[j,a,b,k,*]

[a] The State Key Laboratory of Brain and Cognitive Science, The University of Hong Kong, Hong Kong, China
[b] Laboratory of Social Cognitive and Affective Neuroscience, The University of Hong Kong, Hong Kong, China
[c] Department of Psychology, School of Public Health, Southern Medical University (Guangdong Provincial Key Laboratory of Tropical Disease Research), China
[d] Department of Psychiatry, Zhujiang Hospital, Southern Medical University, Guangzhou 510282, China
[e] Department of Rehabilitation Sciences, The Hong Kong Polytechnic University, Hong Kong, China
[f] Department of Psychiatry and Psychotherapy, Medical University of Vienna, Austria
[g] Department of Radiology, The Affiliated Hospital of Guangzhou Medical University (Guangzhou Huiai Hospital), China
[h] Department of Psychiatry, The Second Affiliated Hospital of Guangzhou Medical University, China
[i] Department of Affective Disorders, The Affiliated Hospital of Guangzhou Medical University (Guangzhou Huiai Hospital), China
[j] Laboratory of Emotion and Cognition, The Affiliated Hospital of Guangzhou Medical University, China
[k] Center for Brain Science and Brain-Inspired Intelligence, Guangdong-Hong Kong-Macao Greater Bay Area, China

ARTICLE INFO

Keywords:
Rumination
Depression
Attentional control
Graph theory
Functional connectivity

ABSTRACT

Background: Rumination is a central feature of major depressive disorder (MDD). Knowledge of the neural structures that underpin rumination offers significant insight into depressive pathophysiology and may help to develop potential intervention strategies for MDD, a mental illness that has become the leading cause of disability worldwide.

Methods: Using resting-state fMRI and graph theory, this study adopted a connectome approach to examine the functional topological organization of the neural network associated with rumination in MDD. Data from 96 participants were analyzed, including 51 patients with MDD and 45 healthy controls.

Results: We found altered functional integration and segregation of neural networks associated with depressive rumination as indicated by reduced global and local efficiency in MDD patients compared with controls. Interestingly, these metrics correlated positively with depression severity, as measured by the Hamilton Depression Rating Scale. Moreover, mediation analysis indicated that the association between network metrics and depression severity was mediated by the ruminative tendency of patients. Disrupted nodal centralities were located in regions associated with emotional processing, visual mental imagery, and attentional control.

Conclusion: Our results highlight rumination as a two-edged sword that reflects a disease-specific neuropathology but also points to a functionality of depressive symptoms with evolutionary meaning.

1. Introduction

Major depressive disorder (MDD) is a considerably disabling mental illness. According to the World Health Organization (WHO, 2017), > 300 million people worldwide suffer from MDD. MDD is associated with an enormous economic cost that ranks as the highest among brain disorders (Smith, 2011). However, knowledge about depressive pathophysiology is still limited. Although it is diagnosed as a single entity, MDD is highly heterogeneous (Uher et al., 2014; Zimmerman et al., 2015). Though it is not recognized in the criteria for MDD, studies indicate that depressive rumination—defined as an uncontrollable and recurrent focus on the depressive state—is a central psychological engine precipitating feature of MDD (Hamilton et al., 2015; Lyubomirsky et al., 2015; Papageorgiou and Wells, 2004). Rumination exacerbates and prolongs depression while predisposing/precipitating depression in vulnerable individuals. Rumination affects depression via four mechanisms (Nolen-Hoeksema et al., 2008). First, rumination increases negative thoughts induced by the depressed

* Correspondence to: Tatia M.C. Lee, Room 656, Laboratory of Neuropsychology, The Jockey Club Tower, The University of Hong Kong, Pokfulam Road, Hong Kong, China.
** Correspondence to: K. Lin: Department of Affective disorder, Guangzhou Brain Hospital, 36 MingxinLoad, Guangzhou, Guangdong Province 510370, China.
E-mail addresses: linkangguang@163.com (K. Lin), tmclee@hku.hk (T.M.C. Lee).

https://doi.org/10.1016/j.pnpbp.2019.109819
Received 23 March 2019; Received in revised form 12 November 2019; Accepted 12 November 2019
Available online 14 November 2019

mood. Second, rumination increases pessimistic and fatalistic thinking and thereby interferes with effective problem-solving. Third, rumination hinders conditioned behavior, which increases stress. Finally, individuals with a ruminative tendency experience less social support, which further intensifies the depressed mood (Watkins, 2008), prolongs depressive episodes (Nolen-Hoeksema et al., 2008), and increases the risk of relapse (Nolen-Hoeksema, 2000).

Although rumination can be regarded a normal variant of cognition, its exaggerated form in depression may be rooted in impaired attention disengagement (Koster et al., 2011; Southworth et al., 2017). Selective attention to task-relevant information is impaired in MDD patients (Koster et al., 2011). Neurophysiological data demonstrate that conflict monitoring decreases with the number of depressive episodes (Vanderhasselt and De Raedt, 2009). Moreover, cognitive training modifies negative attention bias and is associated with changes at the neural level, as well as the clinical level (Beevers et al., 2015). Importantly, the neural basis of depressive rumination may represent trait-based risk factors for relapse in MDD. For example, Jacobs et al. (2014) found that functional connectivity strength between the subgenual anterior cingulate and posterior cingulate gyrus correlated negatively with rumination in remitted MDD. Peters et al. (2016) found that the functional connectivity between the amygdala and the posterior cingulate cortex mediates the association between rumination and residual clinical symptoms in remitted MDD. Thus, studying the neural basis of depressive rumination provides important insights into the mechanisms predisposing and maintaining MDD (Holmes and Patrick, 2018) and may guide the development of new treatments (Young and Craske, 2018).

Recent advances in functional neuroimaging methodology—in particular, the analysis of the brain connectome using graph theory—allow for the characterization of the functional organization of brain networks at different levels of complexity (Bullmore and Bassett, 2011; Fadok et al., 2018). By modeling the brain as a connectome, topological network metrics defined by graph theory can test if the interaction between neural populations is optimal or redundant (Vecchio et al., 2017). These metrics include functional segregation (how optimized the network is for specialized processing) and functional integration (how well the network can combine specialized information across distributed regions Sporns et al., 2004). Thus, examining network properties using graph theory may help to differentiate the neural networks associated with depressive rumination in MDD patients from those associated with rumination in healthy controls (HCs; Bi and He, 2014).

Rumination involves a broad range of cognitive and affective processes including self-referential processing, autobiographical memories, and emotion regulation (Cooney et al., 2010; Sin et al., 2018). Rumination thus activates a distributed and partly overlapping network of brain regions serving these processes. The default mode network (DMN) includes the ventral-medial prefrontal cortex and posterior cingulate gyrus extending to the precuneus and medial temporal gyrus, and it is implicated in self-referential processing (Raichle, 2015). Indeed, Cooney et al. (2010) demonstrated significantly stronger neural activity in the DMN during rumination in MDD patients compared to HCs. Significant neural correlates of rumination apart from the DMN include task-positive networks (e.g., fronto-parietal network) and the amygdala. Hamilton et al. (2011) reported that task-positive networks were associated with rumination in people with MDD. Levels of self-reported rumination were also positively correlated with sustained activation of the amygdala in response to emotional stimuli in people with MDD (Burkhouse et al., 2017). Cooney et al. (2010) reported significantly stronger activation of the amygdala in MDD patients compared to controls during experimentally induced rumination. Kühn et al. (2012) found that depressive rumination correlated negatively with gray matter density and resting state activity in the inferior frontal gyrus and anterior cingulate cortex. Interestingly, Connolly et al. (2013) found the above-mentioned two regions show lower resting state functional connectivity, which is associated with ruminative tendency in adolescents with a first-episode depression. Furthermore, Piguet et al. (2014) found that subjects with high ruminative tendency have more spontaneous neural activity in the left entorhinal region, a key region for memory. Taken together, previous studies point to a link between rumination and DMN, with an imbalance between the recruitment of externally directed attention/executive control networks (in fronto-parietal cortices) and internally directed self-referential/memory networks (in midline and limbic brain systems). However, the organization and interaction on a network level of brain areas associated with depressive rumination remains to be investigated.

This study examined the functional topological organization profile of the neural network of rumination in MDD using resting state functional magnetic resonance imaging (fMRI) and graph theory. First, we defined a neural network based on rumination-induced brain activation, as done previously (Burkhouse et al., 2017; Cooney et al., 2010). We then used graph theory to estimate the topological properties of the rumination network at a regional and a global level by applying the identified nodes of the rumination network to the resting-state fMRI data. Finally, we assessed the association between topological properties and clinical variables (e.g., ruminative tendency and depression severity). We hypothesized that there would be alterations in the functional integration and segregation of the rumination network in MDD patients compared to HCs. Furthermore, we hypothesized that the alterations would correlate with the severity of the depressive symptoms and that these correlations are mediated by depressive rumination.

2. Material and methods

2.1. Participants

The initial sample consisted of 100 right-handed participants including 53 patients with MDD and 47 sex- and age-matched HCs. Patients were diagnosed according to DSM-5 criteria (Uher et al., 2014) by their case psychiatrists (KGL, YD, and XJH). All of the patients had 17 or more scores on the HAMD-21 (Cusin et al., 2009). The exclusion criteria were patients with other psychiatric disorders (except for MDD), a history of organic brain disorder, neurological disorders, mental retardation, cardiovascular diseases, alcohol or substance abuse, pregnancy, or any physical illness. None of them had received electroconvulsive therapy within six months prior to data collection. For study inclusion, patients were diagnosed and screened by a psychiatrist and were scanned within one week after inclusion. Most patients (36/53) experienced chronic illness duration ($>$ 12 months) and all patients received antidepressant pharmacological treatment (see Table 1) at least 7 days prior to inclusion.

HCs were recruited through local advertisements and screened using the Structured Clinical Interview for *DSM5* Nonpatient Edition to rule out the presence of current or past psychiatric disorders. Further exclusion criteria for HCs were any history of psychiatric disorders in first-degree relatives and current or past significant medical or neurological illness. Ethical approval was obtained from the Institutional Review Board of the Guangzhou Brain Hospital. All experimental procedures were conducted according to the Declaration of Helsinki.

All the participants were right-handed according to their self-reporting and had no brain abnormalities according to conventional MRI by an experienced radiologist (WJZ). All the subjects gave written consent prior to study inclusion and were compensated for their participation (¥ 150).

2.2. Psychometric measures

Depressive symptoms were assessed using the 21-item version of the Hamilton Depression Rating Scale (HAMD-21) on the day of the fMRI measurement. Participants also completed the Ruminative Response

Table 1
Demographic and clinical characteristics of MDD and HC.

	MDD Mean (SD)	HC Mean (SD)	t/X2, p
Age	31.9 (9.96)	28.93 (10.88)	$t = 1.43, p = .15$
Sex	31F/22M	27 F/20 M	$X^2 = 0.03, p = .85$
Years of education	12.88 (3.51)	13.46 (3.16)	$t = -0.87, p = .38$
HAMD	33.59 (8.17)	2.10 (3.57)	***t = 24.43, p < .001***
HAMA	18.61 (7.63)	1.44 (2.68)	***t = 14.64, p < .001***
RRS total	57.42 (11.26)	37.53 (9.23)	***t = 9.61, p < .001***
RRS depressive	30.74 (6.65)	18.95 (5.15)	***t = 9.84, p < .001***
RRS brooding	14.59 (3.03)	9.57 (2.66)	***t = 8.77, p < .001***
RRSpondering	11.91 (3.04)	9 (2.38)	***t = 5.27, p < .001***
Stroop-Congruent			
Reactions time	1043 (197)	1131(183)	***t = 2.12, p = .03***
Accuracy	0.76 (0.18)	0.85 (0.14)	***t = −2.48,p = .01***
Stroop-Incongruent			
Reaction time	1229 (192)	1101 (215)	***t = 2.96, p = .003***
Accuracy	0.78 (0.22)	0.87 (0.14)	***t = −2.28,p = .02***
Illness duration (months)	33.70 (36.54)		
Medication (N)			
SSRI	40		
Antipsychotics	13		
Traditional Chinse Medicine	3		
Other	2		

Notes: MDD, major depressive disorder; HC, healthy controls; SD, standard deviation; HAMD/HAMA, Hamilton Depression Rating Scale/Hamilton anxiety scale; RRS, ruminative response scale; SSRI, selective serotonin reuptake inhibitor.
Bold and italic font indicates the areas showing group differences between MDD and HC.

Scale (RRS), a self-assessment widely used to measure ruminative tendency (Treynor et al., 2003). The Chinese version of RRS was used (Han and Yang, 2009). Moreover, all participants completed a computer version of the Stroop color word task to determine participants' interference-control ability as described previously (Zhang et al., 2017).

2.3. Imaging data acquisition and preprocessing

All neuroimaging data were acquired on a 3 Tesla MRI system (Achieva X-series, Philips Medical Systems, Best, Netherlands) using an eight-channel SENSE head coil at the Guangzhou Brain Hospital Department of Radiology.

BOLD-weighted fMRI images were acquired using a gradient-echo echo-planar imaging (GRE-EPI) sequence with (a) repetition time = 2000 ms, (b) echo time = 30 ms, (c) flip angle = 90°, (d) matrix = 64 × 64, (e) field of view = 220 mm × 220 mm, (f) slice thickness = 4 mm with interslice gap = 0.6 mm, and (g) 33 interleaved axial slices. The resting state fMRI consisted of 240 volumes obtained in about 8 min. During the resting fMRI scanning, all lights in the scanner room were switched off, and the subjects were instructed to close their eyes, to keep still, and not to think about anything but also not to fall asleep. In addition, T1-weighted images were acquired with an interleaved sequence (188 sagittal slices, TR/TE/flip angle = 8.2 ms/3.7 ms/7°, matrix = 256 × 256 mm^2, FOV = 256 × 256 × 188 mm, and voxel size = 1 × 1 × 1 mm^3).

The BOLD fMRI data were preprocessed using SPM12 (http://www.fil.ion.ucl.ac.uk/spm/) and DPARSF (V4.3_170105, Yan, 2014). The first five volumes of each dataset were discarded to allow for MR signal equilibrium. The remaining images were corrected for slice timing differences, realigned to the first volume, and spatially normalized to a standard EPI template (Calhoun et al., 2017). Further preprocessing steps included resampling to a voxel size of 3 × 3 × 3 mm^3, linear detrending and temporal band-pass filtering (0.01–0.08 Hz), and smoothing with a 6 mm Gaussian kernel. Moreover, we regressed out the Friston-24 parameters of head motion (six head motion parameters, six head motion parameters one time point before, and the twelve corresponding squared items; (Power et al., 2012; Satterthwaite et al., 2013) and the signals of the white matter and cerebrospinal fluid. With respect to global signals, we referred to the Global Negative Index (GNI) (Chen et al., 2012) to determine whether global signal regression was needed for the current study. This index recommends against performing global signal regression analysis when GNI is 3 or above. After examination of GNI profiles, which were estimated using the publicly available Matlab code (by Chen Gang, https://www.mathworks.com/matlabcentral/fileexchange/36864-determine-the-necessity-for-global-signal-regression), we found all participants had a GNI > 3. Furthermore, a *t*-test revealed no significant difference between MDD patients and HCs ($p = .18$). We thus refrained from performing global signal regression analysis in our preprocessing analysis given the risk of introducing bias (e.g., Weissenbacher et al., 2009). The GNI profile of each subject can be found in Fig. S4a in the Supplement. Regarding head motion on the signal, two steps were adopted to largely extend controlling the effects of head motion. First, if Power frame displacement was found to be > 0.5, then that time point was deemed a "bad" time point, and the time points before and after that bad time point were scrubbed using each of the bad time points as a regressor (Power et al., 2012). Furthermore, a *t*-test revealed no significant difference in mean frame displacement (FD) between the two groups ($p = .18$, Fig. S4 in the Supplement). Correlation analysis also did not find any significant relationship between the FD and self-reported rumination scores ($p > .05$). Second, only if the subjects satisfied our criteria for head motion, displacement of < 3 mm in any plane and rotation of < 3° in any direction were included. Four participants were excluded because of motion artifacts. Hence, a total of 51 MDD patients and 45 age- and gender-matched HC subjects were entered into the final data analysis.

2.4. Rumination network construction and analysis

2.4.1. Node definition

Power et al. (2012) proposed that a functional atlas is a more powerful approach than that based on an anatomical atlas approach in detecting the dynamic functional organization of the rumination network. Following this line of thought, we defined the ruminative neural network based on the activation map of a rumination induction task (Burkhouse et al., 2017; Cooney et al., 2010). Participants had to briefly engage in a state of rumination by means of mood induction and rumination induction instructions (detailed information on the rumination-induction task can be found in the Supplement).

General linear modeling method was applied to delineate the activation patten of the rumination condition so as to further understand the ruminative network on the basis of the activation pattern elicited by the rumination induction task. We built nonoverlapping spheres around each peak voxel in the map (Ekman et al., 2012; Xu et al., 2016). Briefly, we started by building the first sphere (radius = 6 mm) around the most significant peak as the first node of the network; we then moved on to the voxel with the second highest value to construct the second sphere. A node was excluded if it overlapped with any of the previously generated nodes or extended beyond the gray matter mask (> 0.4, mask provided by SPM12). This process was iterated until the last voxel in the activation map and resulted in 49 regions of interest (ROIs). In addition, previous work suggested that the anterior cingulate gyrus and amygdala play an essential role in distinguishing the rumination state from other mental states (Milazzo et al., 2014). Therefore, we also included the bilateral anterior cingulate (4, 31, −10 and − 4, 31, −10) following previous work (Craddock et al., 2009) and the bilateral central-medial amygdala as defined by cytoarchitectonic mapping (Amunts et al., 2005). Since the imaging data of eight subjects did not cover the whole cerebellum in the resting state scan, we only defined ROIs in the cerebral cortex. In total, 53 ROIs (spheres of 6 mm

radius around the most significant peak voxels) were defined to represent the nodes of the rumination network (see Table S3).

2.4.2. Edge definition

We extracted the time series for each ROI by averaging the time course of included voxels. A linear regression analysis was performed to remove the effects of nuisance signals from white matter, cerebrospinal fluid, and head-motion parameters. Subsequently, we used the residuals of the time series for each ROI to calculate a Pearson's correlation coefficient as the functional connectivity. To enhance data distributions for a parametric statistical analysis, Fisher r-to-z transformation was performed. Thus, a 53 × 53 functional connectivity matrix was derived of each subject, representing the rumination network under resting state. The whole procedure of functional connectome construction is shown in Fig. S5 in the Supplement.

2.4.3. Graph theory analysis

Graph theoretical analysis was done using the GRETNA toolbox (Wang et al., 2015a, 2015b) in Matlab (R2015a). We evaluated the rumination network's functional network organization at the level of functional segregation and functional integration (Sporns, 2013). Functional segregation is characterized by the clustering coefficient (*Cp*) and by local efficiency (E_{loc}), whereas functional integration is measured by the characteristic path length (average shortest path length, *Lp*) and global efficiency (E_{glob}). For an estimate of nodal centralities, we characterized nodal strength (S_i), regional global efficiency (E_{nod}), and the regional clustering coefficient (C_i). Moreover, we estimated the small-world attributes (σ) that reflect an optimal balance of integration and segregation of a network. The formula of each metric is depicted in the Supplement or in Rubinov and Sporns (2010).

2.5. Statistical analysis

We used a nonparametric permutation test to assess differences in network parameters between groups (Yang et al., 2017; Zhang et al., 2015). Cohen's *d* was calculated to determine effect sizes. Moreover, connectivity matrices of each group were entered into the Network-Based Statistics (NBS) Toolbox including age and gender as nuisance variables (Zalesky et al., 2010). Connections with *p* values passing a significant nonzero threshold ($p < .01$, Bonferroni corrected) in each group were preserved and a union mask was generated that covered all significant connections in either group. The primary threshold of the individual-connection level was set at $p < .01$ with an extent-based correction for multiple comparisons, 10,000 permutations, and an overall corrected $\alpha < 0.05$. Connectivity components showing differences between MDD patients and HCs, including those identified by NBS, were subjected to a linear regression analysis to investigate their relationship with clinical variables of depression severity, rumination tendency, and cognitive performance. In addition, we performed a mediation analysis (the *mediation* package as implemented in the statistical software R) to determine whether the relationship between network metrics and depression severity is mediated by the ruminative tendency of patients.

2.6. Evaluation of network properties using whole-brain data

To determine whether the results were confined to the selection of nodes defined by the rumination-induction task, we reran the same analysis using 142 ROIs (Dos atlas) covering most of the brain (excluding the cerebellum) as defined previously (Dosenbach et al., 2010). It is noteworthy that 42 ROIs defined from the rumination-induction task overlapped with the Dos atlas (see Table S3 in Supplementary).

3. Results

3.1. Demographic and behavioral data

Demographic data are depicted in Table 1. No significant differences were observed between MDD patients and HCs in demographic variables including gender, age, or years of education ($P > .05$). As expected, patients had significantly higher scores in the HAMD and RRS and exhibited significantly longer reaction times and lower accuracy rates in the Stroop task compared to HCs ($Ps < .05$).

3.2. Neural correlates of rumination

The rumination-induction task successfully induced rumination in all participants as indicated by higher self-sadness and self-focus under the rumination condition ($p < .05$, see Fig. S2 in the Supplement). Furthermore, rumination induction was associated with significant activation in the bilateral middle occipital gyri extending to the cerebellum, the bilateral inferior parietal lobule, the right inferior frontal gyrus extending to the insula, and subcortical areas including the parahippocampus, thalamus, and amygdala (see Fig. S3 in the Supplement). These findings are in line with that observed in previous studies (Burkhouse et al., 2017; Cooney et al., 2010) and add to the literature on the neural network underpinning rumination.

3.3. Altered network metrics in MDD patients

The rumination network derived from the activation patterns of the rumination-induction task as described above exhibited small-worldness ($\sigma > 1$) in both groups (Fig. S6 in the Supplement) across a wide range of density from 0.15 to 0.45. Group comparisons demonstrated that MDD patients exhibited a decreased clustering coefficient (C_p,$p = .037$, Cohen $d = 0.36$), a decreased local (E_{loc}, $p = .029$, Cohen $d = 0.40$) and global efficiency (E_{glob},$p = .013$, Cohen $d = 0.47$), and an increased characteristic path length (L_p,$p = .006$, Cohen $d = 0.52$) compared to HCs (Fig. 1).

Examining group differences at the regional level revealed decreases in nodal strength, nodal efficiency, and the nodal clustering coefficient in MDD patients in the bilateral amygdala, the right precuneus, the middle occipital gyrus, the left inferior parietal lobule, and the right superior parietal lobule. In only one region, the right middle frontal gyrus, was there an increase in the nodal-clustering coefficient in MDD patients compared to HCs (Table 2 and Fig. 2). Areas identified as hub nodes in controls but not in patients included the right precuneus and right inferior parietal lobe (Fig. 2).

The NBS analysis revealed 50 links displaying a decreased functional connectivity in MDD patients compared with HCs ($p = .0371$; Table S4 & FigureS7a in the Supplement). Reduced connectivity was found in the frontal limbic circuits, including the inferior frontal gyrus, amygdala, putamen, and regions of the DMN, such as the middle temporal gyrus, precuneus, and areas in the occipital and parietal lobes. Affected connections tended to interconnect different functional systems (e.g., parietal-occipital, frontal-occipital, and occipital-subcortical). The functional connectivity strength from the links identified by NBS showing as decreased in MDD patients were significantly correlated with global network metrics (i.e., E_{glob}, E_{loc}, and L_p) exhibiting group differences in the MDD group ($Ps < .05$, Fig. S7 b, c, & d in the Supplement).

3.4. Relationship between connectivity metrics and clinical scores

Ruminative tendency (RRS total scores and RRS pondering scores) showed a significant positive association with HAMD scores (Table S5 and Fig. S8 in the Supplement). Moreover, HAMD scores, RRS total scores, and RRS pondering scores correlated positively with global network metrics exhibiting decreases in MDD patients (i.e., C_p, E_{loc},

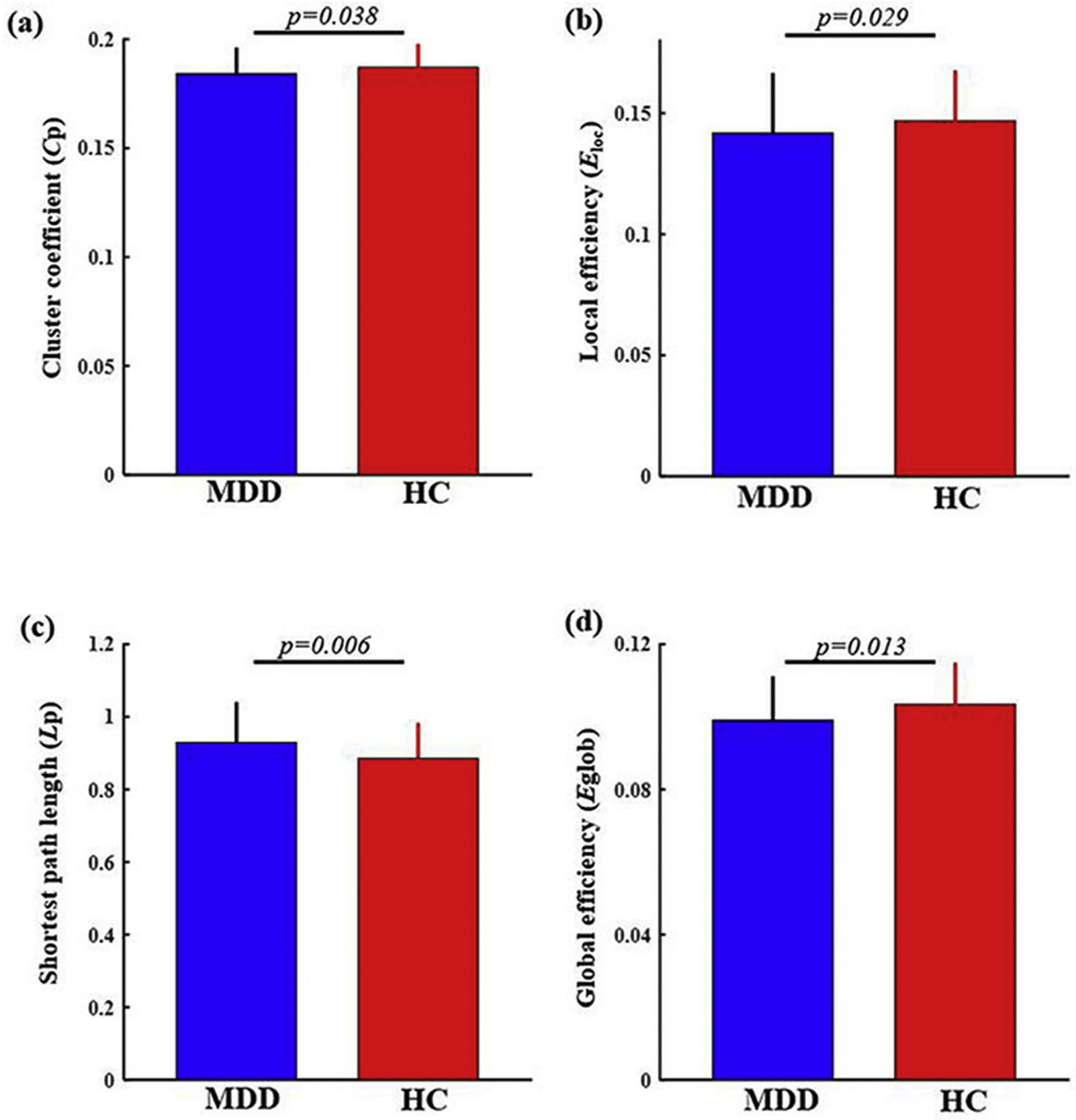

Fig. 1. Global network metrics of ruminative neural network. (a, b, c, and d) The area of curve of network metrics, clustering coefficient (C_p), local efficiency (E_{loc}), shortest path length (L_p), global efficiency (E_{glob}), respectively. The error bar indicates ± 1 standard error.

E_{glob}, and L_p, *Ps* < .05). In comparison, a negative correlation existed between HAMD scores and the characteristic path length (*Ps* < .05, Table S5 in the Supplement), a metric that increased in MDD patients compared to HCs. Mediation analysis (Baron and Kenny, 1986) revealed that ruminative tendency, especially pondering, mediated the association between network metrics and HAMD (Fig. 3 and Fig. S8 in Supplement). First, the proposed mediator of reflective pondering was regressed on global network metrics. Indeed, global metrics could significantly predict reflective pondering. Second, HAMD scores were regressed on global network metrics, demonstrating that global network metrics significantly predicted HAMD scores. Finally, HAMD scores were regressed on global network metrics and reflective pondering within the same regression model. Reflective pondering significantly predicted HAMD, whereas the association between global network metrics and HAMD decreased in strength in the presence of the mediator (all *Ps* < .05). Thus, mediation analysis demonstrated that reflective pondering partially mediates the association between global metrics and HAMD scores.

No significant correlations were observed between cognitive performance (i.e., reaction time and accuracy rate in Stroop task) and network metrics, or between the duration/number of illness episodes and network metrics (Table S5 in the Supplement).

3.5. Evaluation on a whole-brain level

No significant between-group differences were observed in global network metrics defined previously as covering 142 nodes across the whole brain (Dosenbach et al., 2010); Fig. S9 in Supplement). This indicates that altered network metrics in MDD patients are confined to networks associated with rumination.

4. Discussion

The results of this study demonstrate alterations in the functional

Table 2
Regions showing significant group differences in the area of cure (AUC) of nodal strength, efficiency and clustering coefficient.

Region	Nodal strength (Si)	*p* (Cohen d) Nodal efficiency	Cluster coefficient
	Nodal strength (S_i)	Nodal efficiency (E_{nod})	Clustering coefficient (C_i)
HC > MDD			
#02-MOG.R	0.065 (0.25)	***0.012 (0.39)***	***0.002 (0.50)***
#05-IPL.L	0.034 (0.37)	***0.013 (0.43)***	0.452 (0.06)
#06-IOG.L	0.054 (0.28)	***0.017 (0.37)***	0.421 (0.04)
#07- ITG.L	0.205 (0.15)	***0.017 (0.40)***	0.075 (0.32)
#08-ITG.L#	***0.009 (0.54)***	***0.002 (0.61)***	0.490 (0.05)
#17-IPL.L	0.024 (0.41)	***0.003 (0.54)***	0.063 (0.26)
#22-SPL.R	0.063 (0.33)	***0.016 (0.42)***	0.135 (0.25)
#31-PCUN.R	0.022 (0.31)	***0.008 (0.39)***	0.371 (0.10)
#33-ITG.R	0.038 (0.41)	***0.008 (0.50)***	0.358 (0.02)
#52-Amy.L	0.266 (0.09)	0.198 (0.19)	***0.006 (0.52)***
#53-Amy.R	***0.005 (0.61)***	***0.001 (0.72)***	0.123 (0.42)
HC < MDD			
#48-MFG.R	0.262 (0.06)	0.101 (0.19)	***0.003 (0.62)***

Notes: Bold and italic font indicates the areas showing group differences between MDD and HC. MOG. R, right middle occipital gyrus; IPL.L, left inferior parietal lobule; IOG.L, left inferior occipital gyrus; ITG.L, left inferior temporal gyrus; ITG.L/R, left/right inferior temporal gyrus; SPL.R, superior parietal lobule; PCUN.R, right precuneus; Amy.L/R, left/right amygdala; MFG.R, right middle frontal gyrus.

organization of the neural network associated with depressive rumination. Compared to HCs, MDD patients exhibited network alterations on a global and local level that were characterized by a deficiency of local information transfer (reduced clustering coefficient) and by weakened functional connections in terms of a reduced segregation and integration (decreased local and global efficiency). Alterations of individual nodes were predominantly found in systems involved in emotional processing, visual mental imagery, and attentional control. However, network metrics in MDD patients positively correlated with the severity of depression as measured with the HAMD. The latter finding apparently contradicts reductions in network metrics and might indicate two separate features of functional network organization that seem to counteract each other: one separates MDD patients from HCs, whereas the other reflects the current depressive state of patients. In the following discussion, we will try to reconcile these conflicting findings.

The rumination-induction task used in our study revealed robust activations in cortical and subcortical regions commonly observed during rumination, including the inferior parietal and inferior frontal regions, the parahippocampus, the thalamus, and the amygdala (Burkhouse et al., 2017; Cooney et al., 2010). Previous studies suggested that rumination assessed by questionnaire (e.g., RRS) showed close association with gray matter density of the parahippocampus and frontal cortex (Wang et al., 2015a, 2015b). Moreover, Peters et al. (2016) found that amygdala-related functional connectivity positively correlated with RRS scores. Our present study revealed that network metrics derived from the ruminative neural network, as well as scores of self-focus during the rumination condition, positively correlated with RRS scores. Taken together, these results indicate that the organization profile of the ruminative neural network consisting of brain areas tapped by rumination state may also reflect unscripted, or trait rumination.

Graph theoretical analysis of the rumination network revealed small-world properties in both groups, which suggests that rumination

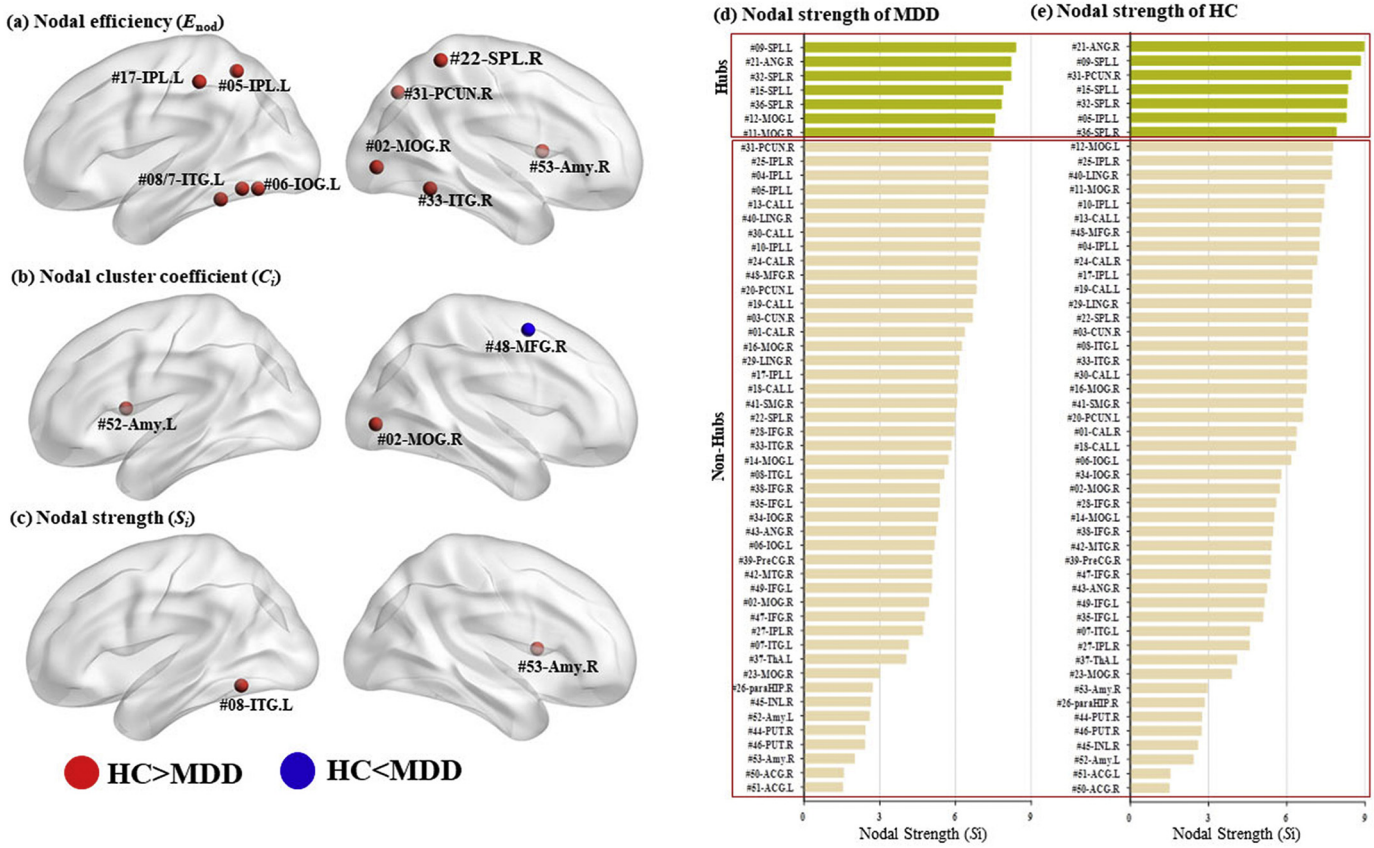

Fig. 2. Group differences in nodal metrics and hubs in each group. (a, b, and c) Nodal metrics nodal efficiency (E_{nod}), nodal clustering coefficient (C_i), and nodal strength (S_i) showing group differences, respectively ($p < .018$, corrected). Note that the node showing an increase in MDD is indicated by blue dots, while colored dots show a decrease in MDD patients compared with HCs; (e, f) Nodal strength of each group. Hubs are coded with dark yellow. The brain display used software developed by Xia et al. (2013). (For interpretation of the references to color in this figure legend, the reader is referred to the web version of this article.)

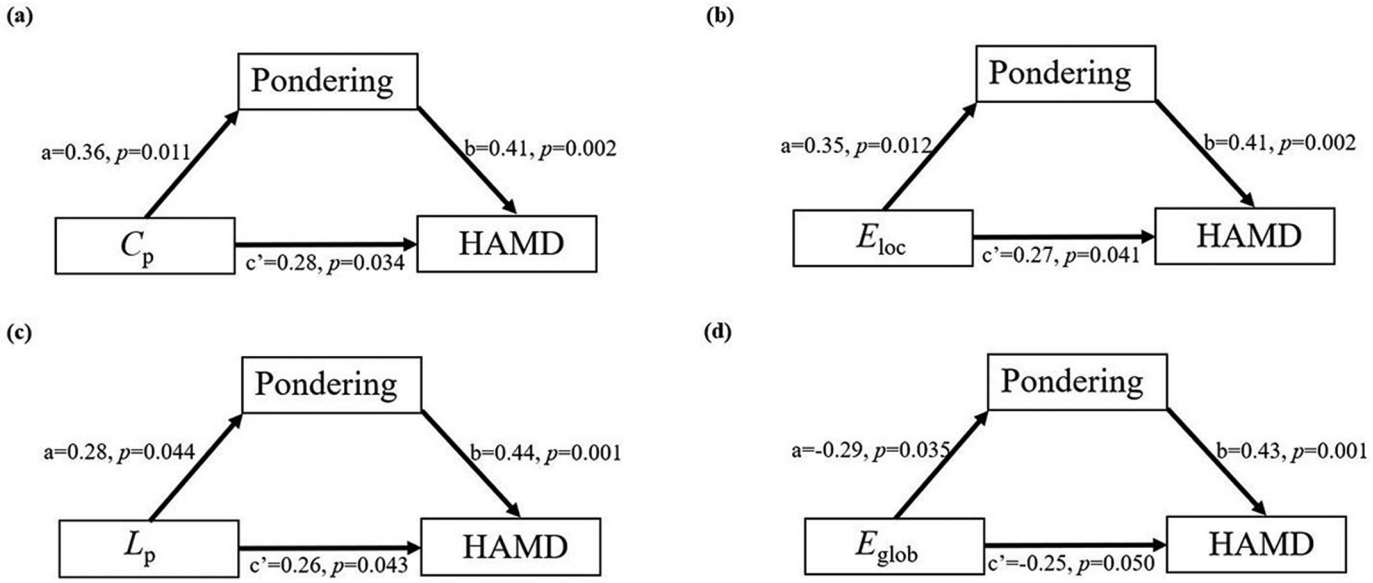

Fig. 3. Model of global metrics as a predictor of depressive severity mediated by reflective pondering. There are significant indirect effects of global metrics on depressive severity measured by the Hamilton depressive rating scale (HAMD) via reflective pondering (a, b, c, and d). Path coefficients and corresponding *p* values are shown next to arrows; path *a* indicates the relationship between global metrics and pondering; path *b* indicates the relationship between pondering and HAMD; path *c* indicates the direct effect of global metrics on the HAMD.

is an independent mental regime with a unique organizational profile (Kennair et al., 2017; Nolen-Hoeksema et al., 2008). However, group comparisons demonstrated alterations in the integrity of the rumination network in MDD patients compared to HCs as indicated by abnormal functional integration and segregation. Compared to HCs, patients with MDD exhibited decreases in local and global efficiency and in the clustering coefficient and increases in characteristic path length. This is in line with a recent study by Wang et al. (2017) who detected decreased global efficiency and increased characteristic path length in MDD as well as bipolar II disorder (Wang et al., 2017). However, other studies revealed opposing results. For instance, Zhang et al. (2011) observed a lower path length and higher global efficiency in first episode drug-naïve MDD patients. Moreover, several studies also found no differences in global topological properties between patients with MDD and HCs (Bohr et al., 2013; Lord et al., 2012; Peng et al., 2014). All of our patients were medicated, but it is unlikely that medication explains this inconsistency given that the results of Wang et al. are in line with ours even though their patients were drug-naïve or unmedicated for at least 5 months prior to measurement (Wang et al., 2017). In order to reconcile these contradictions, it is important to note that Zhang et al. (2011) investigated first-episode major depression whereas our patients as well as the patients in Wang et al. (2017) were ill for an average of 34 and 41 months, respectively. Indeed, most of our patients (36/53) experienced chronic illness duration (> 12 months) and all patients received antidepressant pharmacological treatment (see Table 1) for at least 7 days prior to study inclusion. Moreover, 15 of our patients were classified as treatment refractory. Hence, HAMD scores in our study may well reflect a degree of treatment resistance and treatment duration. Furthermore, our current study focused on a functional connectome defined by nodes based on a rumination induction task, which is a quite different approach compared to previous studies that covered the whole brain (Bohr et al., 2013; Lord et al., 2012; Peng et al., 2014; Wang et al., 2017; Zhang et al., 2011). Hence, factors pertaining to illness duration, including adaptations on a behavioral and neural level, sample difference, and methodological differences in constructing networks may be considered in explaining these discrepancies.

Neural adaptation may also explain the positive correlation between global network metrics and depression severity. If observed reductions in network metrics in MDD patients are not the cause of the disorder but rather an adaptive process in response to the disorder, then it is conceivable that the adaptation process is signaled by depression severity. In other words, depression severity may decline the more adapted a neural network is. Moreover, mediation analysis indicated that rumination, especially reflective pondering, mediated the relationship between network features and depression severity. Indeed, such mediation by rumination may be expected, since network nodes were based on rumination-induced neural activations. However, our mediation analysis also points to a functionality and usefulness of rumination with evolutionary meaning. Such an adaptation might have evolved in order to sustain analysis of complex problems and eventually overcome the depressive mode in patients (Andrews and Thomson Jr, 2009).

Focusing on the regional metrics, nodal centralities in the bilateral amygdala exhibited a significant decrease in MDD patients compared with HCs. The amygdala is a pivotal area responsible for regulating internal emotional states leading to appropriate behavior (Fadok et al., 2018). Furthermore, rumination is generally triggered by internal (e.g., negative affect) or external events that conflict with an individual's goals (Koster et al., 2011) and that are further processed by a visual imagery system (Renner et al., 2017). Indeed, visual mental imagery is more vivid in patients with MDD, which is also reflected by a stronger recruitment of visual and somatic brain regions compared to HCs (Burkhouse et al., 2017). This is in line with the current results, showing altered nodal centralities in regions within the occipital lobe, such as the left inferior occipital gyrus and the right middle inferior occipital gyrus. Altered nodal centralities were also found in the parietal lobe, including the left inferior parietal lobule, the right superior parietal gyrus, and the right precuneus. These regions govern processes related to attentional control (Dosenbach et al., 2007; Zhang et al., 2017). A core hypothesis of rumination is “impaired attention disengagement” (Koster et al., 2011), which places an individual at risk for ruminative tendency. Moreover, the only region exhibiting increased nodal centrality in the current study is the right middle frontal gyrus, which is a core area of the DMN (Raichle, 2015; Whitfield-Gabrieli and Ford, 2012). Dominance of the DMN that reflects passive self-relational processes, such as autobiographical memory recall and a wandering mind, is a key characteristic of maladaptive and depressive rumination (Hamilton et al., 2015). Thus, current findings may yield important insights into new psychotherapeutic interventions for MDD including

selective attention training and visual mental-imagery training.

Several limitations of our study deserve mention. First, due to time constraints on fMRI studies, our experimental rumination task was not designed to distinguish the fine differentiation of subdomains of rumination (e.g., reflective pondering vs. brooding). Second, the current patient sample was not medication naïve. Hence, we cannot exclude the possibility that treatment partly affected our results. Third, a recent study found that decreased functional connectivity within the DMN is partly associated with the process of mind-wandering and depressive rumination (Rosenbaum et al., 2017). Thus, future studies on the neurophysiological correlates of depressive rumination should assess spontaneous and induced rumination during the rsfMRI scanning. Fourth, our study was cross-sectional in nature, precluding us from testing the hypothesis that network metrics reflect an adaptive process of disease progression. Future studies should compare drug-naïve first-episode and unmedicated recurrent MDD patients in order to find more definite answers. Last but hardly the least, we were unable to implement structured interviews to establish clinical diagnoses for our clinical participants due to resource constraints. We acknowledge that there could be potential confounding variance introduced by classifying our clinical participants based on semi-structured interviews. Future studies should consider employing structured interviews that will provide valid and reliable clinical information.

5. Conclusions

In conclusion, our study demonstrates alterations in the functional organization of the neural network associated with depressive rumination. These alterations may indicate a neural adaptation to the disorder, an adaptation that is inversely related to the severity of depressive symptoms. This severity is mediated by rumination. Our data therefore encourage viewing the role of rumination in depression as a two-edged sword that reflects a disease-specific neuropathology but also points to a functionality of depressive symptoms with evolutionary meaning.

Ethical statement

All relevant ethical safeguards have been met in relation to patient or subject protection, or animal experimentation.

Declaration of Competing Interest

The authors report no biomedical financial interests or potential conflicts of interest.

Acknowledgement

This study was supported by The University of Hong Kong May Endowed Professorship in Neuropsychology, the Science and Technology Program of Guangdong (2018B030334001), the National Natural Science Foundation of China (NSFC: 81671347 and 31900806), and the National Key R&D Program of China (2016YFC1306702).

References

Amunts, K., Kedo, O., Kindler, M., Pieperhoff, P., Mohlberg, H., Shah, N., Habel, U., Schneider, F., Zilles, K., 2005. Cytoarchitectonic mapping of the human amygdala, hippocampal region and entorhinal cortex: intersubject variability and probability maps. Anat. Embryol. 210 (5-6), 343–352.

Andrews, P.W., Thomson Jr., J.A., 2009. The bright side of being blue: depression as an adaptation for analyzing complex problems. Psychol. Rev. 116 (3), 620.

Baron, R.M., Kenny, D.A., 1986. The moderator–mediator variable distinction in social psychological research: conceptual, strategic, and statistical considerations. J. Pers. Soc. Psychol. 51 (6), 1173.

Beevers, C.G., Clasen, P.C., Enock, P.M., Schnyer, D.M., 2015. Attention bias modification for major depressive disorder: effects on attention bias, resting state connectivity, and symptom change. J. Abnorm. Psychol. 124 (3), 463.

Bi, Y., He, Y., 2014. Connectomics reveals faulty wiring patterns for depressed brain. Biol. Psychiatry 76 (7), 515–516.

Bohr, I.J., Kenny, E., Blamire, A., O'Brien, J.T., Thomas, A., Richardson, J., Kaiser, M., 2013. Resting-state functional connectivity in late-life depression: higher global connectivity and more long distance connections. Front Psychiatry 3, 116.

Bullmore, E.T., Bassett, D.S., 2011. Brain graphs: graphical models of the human brain connectome. Annu. Rev. Clin. Psychol. 7, 113–140.

Burkhouse, K.L., Jacobs, R.H., Peters, A.T., Ajilore, O., Watkins, E.R., Langenecker, S.A., 2017. Neural correlates of rumination in adolescents with remitted major depressive disorder and healthy controls. Cogn. Affect. Behav. Neurosci. 17 (2), 394–405.

Calhoun, V.D., Wager, T.D., Krishnan, A., Rosch, K.S., Seymour, K.E., Nebel, M.B., Mostofsky, S.H., Nyalakanai, P., Kiehl, K., 2017. The impact of T1 versus EPI spatial normalization templates for fMRI data analyses. Hum. Brain Mapp. 38 (11), 5331–5342.

Chen, G., Chen, G., Xie, C., Ward, B.D., Li, W., Antuono, P., Li, S.J., 2012. A method to determine the necessity for global signal regression in resting-state fMRI studies. Magn. Reson. Med. 68 (6), 1828–1835.

Connolly, C.G., Wu, J., Ho, T.C., Hoeft, F., Wolkowitz, O., Eisendrath, S., Frank, G., Hendren, R., Max, J.E., Paulus, M.P., 2013. Resting-state functional connectivity of subgenual anterior cingulate cortex in depressed adolescents. Biol. Psychiatry 74 (12), 898–907.

Cooney, R.E., Joormann, J., Eugène, F., Dennis, E.L., Gotlib, I.H., 2010. Neural correlates of rumination in depression. Cogn. Affect. Behav. Neurosci. 10 (4), 470–478.

Craddock, R.C., Holtzheimer, P.E., Hu, X.P., Mayberg, H.S., 2009. Disease state prediction from resting state functional connectivity. Magn. Reson. Med. 62 (6), 1619–1628.

Cusin, C., Yang, H., Yeung, A., Fava, M., 2009. Rating Scales for Depression, Handbook of Clinical Rating Scales and Assessment in Psychiatry and Mental Health. Springer, pp. 7–35.

Dosenbach, N.U., Fair, D.A., Miezin, F.M., Cohen, A.L., Wenger, K.K., Dosenbach, R.A., Fox, M.D., Snyder, A.Z., Vincent, J.L., Raichle, M.E., 2007. Distinct brain networks for adaptive and stable task control in humans. Proc. Natl. Acad. Sci. 104 (26), 11073–11078.

Dosenbach, N.U., Nardos, B., Cohen, A.L., Fair, D.A., Power, J.D., Church, J.A., Nelson, S.M., Wig, G.S., Vogel, A.C., Lessov-Schlaggar, C.N., 2010. Prediction of individual brain maturity using fMRI. Science 329 (5997), 1358–1361.

Ekman, M., Derrfuss, J., Tittgemeyer, M., Fiebach, C.J., 2012. Predicting errors from reconfiguration patterns in human brain networks. Proc. Natl. Acad. Sci. 109 (41), 16714–16719.

Fadok, J.P., Markovic, M., Tovote, P., Lüthi, A., 2018. New perspectives on central amygdala function. Curr. Opin. Neurobiol. 49, 141–147.

Hamilton, J.P., Furman, D.J., Chang, C., Thomason, M.E., Dennis, E., Gotlib, I.H., 2011. Default-mode and task-positive network activity in major depressive disorder: implications for adaptive and maladaptive rumination. Biol. Psychiatry 70 (4), 327–333.

Hamilton, J.P., Farmer, M., Fogelman, P., Gotlib, I.H., 2015. Depressive rumination, the default-mode network, and the dark matter of clinical neuroscience. Biol. Psychiatry 78 (4), 224–230.

Han, X., Yang, H., 2009. Chinese version of Nolen-Hoeksema ruminative responses scale (RRS) used in 912 college students: reliability and validity. Chin. J. Clin. Psychol. 17 (5), 549–551.

Holmes, A.J., Patrick, L.M., 2018. The myth of optimality in clinical neuroscience. Trends Cogn. Sci. 22 (3), 241–257.

Jacobs, R.H., Jenkins, L.M., Gabriel, L.B., Barba, A., Ryan, K.A., Weisenbach, S.L., Verges, A., Baker, A.M., Peters, A.T., Crane, N.A., 2014. Increased coupling of intrinsic networks in remitted depressed youth predicts rumination and cognitive control. PLoS One 9 (8), e104366.

Kennair, L.E.O., Kleppestø, T.H., Larsen, S.M., Jørgensen, B.E.G., 2017. Depression: Is Rumination Really Adaptive? The Evolution of Psychopathology. Springer, pp. 73–92.

Koster, E.H., De Lissnyder, E., Derakshan, N., De Raedt, R., 2011. Understanding depressive rumination from a cognitive science perspective: the impaired disengagement hypothesis. Clin. Psychol. Rev. 31 (1), 138–145.

Kühn, S., Vanderhasselt, M.-A., De Raedt, R., Gallinat, J., 2012. Why ruminators won't stop: the structural and resting state correlates of rumination and its relation to depression. J. Affect. Disord. 141 (2), 352–360.

Lord, A., Horn, D., Breakspear, M., Walter, M., 2012. Changes in community structure of resting state functional connectivity in unipolar depression. PLoS One 7 (8), e41282.

Lyubomirsky, S., Layous, K., Chancellor, J., Nelson, S.K., 2015. Thinking about rumination: the scholarly contributions and intellectual legacy of Susan Nolen-Hoeksema. Annu. Rev. Clin. Psychol. 11, 1–22.

Milazzo, A.-C., Ng, B., Jiang, H., Shirer, W., Varoquaux, G., Poline, J.B., Thirion, B., Greicius, M.D., 2014. Identification of mood-relevant brain connections using a continuous, subject-driven rumination paradigm. Cereb. Cortex 26 (3), 933–942.

Nolen-Hoeksema, S., 2000. The role of rumination in depressive disorders and mixed anxiety/depressive symptoms. J. Abnorm. Psychol. 109 (3), 504.

Nolen-Hoeksema, S., Wisco, B.E., Lyubomirsky, S., 2008. Rethinking rumination. Perspect. Psychol. Sci. 3 (5), 400–424.

Organization, W.H, 2017. Depression and Other Common Mental Disorders: Global Health Estimates.

Papageorgiou, C., Wells, A., 2004. Depressive Rumination: Nature, Theory and Treatment. John Wiley & Sons.

Peng, D., Shi, F., Shen, T., Peng, Z., Zhang, C., Liu, X., Qiu, M., Liu, J., Jiang, K., Fang, Y., 2014. Altered brain network modules induce helplessness in major depressive disorder. J. Affect. Disord. 168, 21–29.

Peters, A.T., Burkhouse, K., Feldhaus, C.C., Langenecker, S.A., Jacobs, R.H., 2016. Aberrant resting-state functional connectivity in limbic and cognitive control

networks relates to depressive rumination and mindfulness: a pilot study among adolescents with a history of depression. J. Affect. Disord. 200, 178–181.
Piguet, C., Desseilles, M., Sterpenich, V., Cojan, Y., Bertschy, G., Vuilleumier, P., 2014. Neural substrates of rumination tendency in non-depressed individuals. Biol. Psychol. 103, 195–202.
Power, J.D., Barnes, K.A., Snyder, A.Z., Schlaggar, B.L., Petersen, S.E., 2012. Spurious but systematic correlations in functional connectivity MRI networks arise from subject motion. Neuroimage 59 (3), 2142–2154.
Raichle, M.E., 2015. The brain's default mode network. Annu. Rev. Neurosci. 38, 433–447.
Renner, F., Ji, J.L., Pictet, A., Holmes, E.A., Blackwell, S.E., 2017. Effects of engaging in repeated mental imagery of future positive events on behavioural activation in individuals with major depressive disorder. Cogn. Ther. Res. 41 (3), 369–380.
Rosenbaum, D., Haipt, A., Fuhr, K., Haeussinger, F.B., Metzger, F.G., Nuerk, H.-C., Fallgatter, A.J., Batra, A., Ehlis, A.-C., 2017. Aberrant functional connectivity in depression as an index of state and trait rumination. Sci. Rep. 7 (1), 2174.
Rubinov, M., Sporns, O., 2010. Complex network measures of brain connectivity: uses and interpretations. Neuroimage 52 (3), 1059–1069.
Satterthwaite, T.D., Elliott, M.A., Gerraty, R.T., Ruparel, K., Loughead, J., Calkins, M.E., Eickhoff, S.B., Hakonarson, H., Gur, R.C., Gur, R.E., 2013. An improved framework for confound regression and filtering for control of motion artifact in the preprocessing of resting-state functional connectivity data. Neuroimage 64, 240–256.
Sin, E.L., Shao, R., Geng, X., Cho, V., Lee, T., 2018. The neuroanatomical basis of two subcomponents of rumination: a VBM study. Front. Hum. Neurosci. 12, 324.
Smith, K., 2011. Trillion-dollar brain drain. Nature Publishing Group.
Southworth, F., Grafton, B., MacLeod, C., Watkins, E., 2017. Heightened ruminative disposition is associated with impaired attentional disengagement from negative relative to positive information: support for the “impaired disengagement” hypothesis. Cognit. Emot. 31 (3), 422–434.
Sporns, O., 2013. Network attributes for segregation and integration in the human brain. Curr. Opin. Neurobiol. 23 (2), 162–171.
Sporns, O., Chialvo, D.R., Kaiser, M., Hilgetag, C.C., 2004. Organization, development and function of complex brain networks. Trends Cogn. Sci. 8 (9), 418–425.
Treynor, W., Gonzalez, R., Nolen-Hoeksema, S., 2003. Rumination reconsidered: a psychometric analysis. Cogn. Ther. Res. 27 (3), 247–259.
Uher, R., Payne, J.L., Pavlova, B., Perlis, R.H., 2014. Major depressive disorder in DSM-5: implications for clinical practice and research of changes from DSM-IV. Depress. Anxiety 31 (6), 459–471.
Vanderhasselt, M.-A., De Raedt, R., 2009. Impairments in cognitive control persist during remission from depression and are related to the number of past episodes: an event related potentials study. Biol. Psychol. 81 (3), 169–176.
Vecchio, F., Miraglia, F., Rossini, P.M., 2017. Connectome: graph theory application on functional brain networks architecture. Clin. Neurophysiol. Pract. 2, 206–213.
Wang, J., Wang, X., Xia, M., Liao, X., Evans, A., He, Y., 2015a. GRETNA: a graph theoretical network analysis toolbox for imaging connectomics. Front. Hum. Neurosci. 9.
Wang, K., Wei, D., Yang, J., Xie, P., Hao, X., Qiu, J., 2015b. Individual differences in rumination in healthy and depressive samples: association with brain structure, functional connectivity and depression. Psychol. Med. 45 (14), 2999–3008.
Wang, Y., Wang, J., Jia, Y., Zhong, S., Zhong, M., Sun, Y., Niu, M., Zhao, L., Pan, J., Huang, L., 2017. Topologically convergent and divergent functional connectivity patterns in unmedicated unipolar depression and bipolar disorder. Transl. Psychiatry 7 (7), e1165.
Watkins, E.R., 2008. Constructive and unconstructive repetitive thought. Psychol. Bull. 134 (2), 163.
Weissenbacher, A., Kasess, C., Gerstl, F., Lanzenberger, R., Moser, E., Windischberger, C., 2009. Correlations and anticorrelations in resting-state functional connectivity MRI: a quantitative comparison of preprocessing strategies. Neuroimage 47 (4), 1408–1416.
Whitfield-Gabrieli, S., Ford, J.M., 2012. Default mode network activity and connectivity in psychopathology. Annu. Rev. Clin. Psychol. 8, 49–76.
Xia, M., Wang, J., He, Y., 2013. BrainNet viewer: a network visualization tool for human brain connectomics. PLoS One 8 (7), e68910.
Xu, Y., Lin, Q., Han, Z., He, Y., Bi, Y., 2016. Intrinsic functional network architecture of human semantic processing: modules and hubs. Neuroimage 132, 542–555.
Yan, C.-G., 2014. DPABI: A Toolbox for Data Processing & Analysis for Brain Imaging.
Yang, X., Liu, J., Meng, Y., Xia, M., Cui, Z., Wu, X., Hu, X., Zhang, W., Gong, G., Gong, Q., 2017. Network analysis reveals disrupted functional brain circuitry in drug-naive social anxiety disorder. NeuroImage. 190, 213–223.
Young, K.S., Craske, M.G., 2018. The cognitive neuroscience of psychological treatment action in depression and anxiety. Curr. Behav. Neurosci. Rep. 5 (1), 13–25.
Zalesky, A., Fornito, A., Bullmore, E.T., 2010. Network-based statistic: identifying differences in brain networks. Neuroimage 53 (4), 1197–1207.
Zhang, J., Wang, J., Wu, Q., Kuang, W., Huang, X., He, Y., Gong, Q., 2011. Disrupted brain connectivity networks in drug-naive, first-episode major depressive disorder. Biol. Psychiatry 70 (4), 334–342.
Zhang, R., Wei, Q., Kang, Z., Zalesky, A., Li, M., Xu, Y., Li, L., Wang, J., Zheng, L., Wang, B., Zhao, J., Zhang, J., Huang, R., 2015. Disrupted brain anatomical connectivity in medication-naïve patients with first-episode schizophrenia. Brain Struct. Funct. 220 (2), 1145–1159.
Zhang, R., Geng, X., Lee, T.M., 2017. Large-scale functional neural network correlates of response inhibition: an fMRI meta-analysis. Brain Struct. Funct. 222 (9), 3973–3990.
Zimmerman, M., Ellison, W., Young, D., Chelminski, I., Dalrymple, K., 2015. How many different ways do patients meet the diagnostic criteria for major depressive disorder? Compr. Psychiatry 56, 29–34.